Cabozantinib inhibits melanoma brain metastasis in vitro

Trond Are Mannsåker
Department of Biomedicine, University of Bergen
Tuyen Hoang
Department of Biomedicine, University of Bergen
Synnøve Nymark Aasen
Department of Biomedicine, University of Bergen
Ole Vidhammer Bjørnstad
Department of Biomedicine, University of Bergen
Himalaya Parajuli
Department of Biomedicine, University of Bergen
Terje Sundstrøm
Department of Neurosurgery, Haukeland University Hospital
Frits Thorsen (Frits.Thorsen@uib.no)
Department of Biomedicine, University of Bergen

Research Article

Keywords: Brain metastasis, melanoma, cabozantinib, apoptosis, PDGF-Ra, IGF-1R, MERTK, DDR1, MAPK pathway and PI3K pathway

Posted Date: July 6th, 2021

DOI: https://doi.org/10.21203/rs.3.rs-681934/v1

Abstract

Background

Melanoma is one of the cancer types that have high potential to metastasise to the brain. Recent advances in targeted therapies and immunotherapies have changed the therapeutical landscape of extra-cranial melanoma. However, few patients with melanoma brain metastases (MBM) respond effectively to recent treatments and new therapeutic strategies are needed. Cabozantinib is a receptor tyrosine kinase (RTK) inhibitor, already approved by FDA for treatment of renal cell carcinoma, medullary thyroid cancer and hepatocellular carcinoma. The drug also targets several of the proteins which are known to be dysregulated in melanomas and may therefore have a potential role in melanoma treatment. In this study, we investigated the effect of cabozantinib on MBM cell growth and migration *in vitro*, and further identified its associated molecular components.

Methods

The anti-tumour activity of cabozantinib was investigated on three human MBM cell lines (H1, H3, H10) developed in our laboratory, through monolayer cell viability assays, tumoursphere experiments, cell migration assays, flow cytometry and caspase 3/7 apoptosis assays, RTK array screening and western blots (WB) to validate the array findings.

Results

Cabozantinib treatment decreased the viability of MBM cell lines both when grown in monolayer cultures and as tumour spheroids. The *in vitro* cell migration was also inhibited, and apoptosis was induced by cabozantinib. The phosphorylated RTKs p-PDGF-Rα, p-IGF-1R, p-MERTK and p-DDR1 were found to be downregulated in the p-RTK array of MBM cells after cabozantinib treatment. These results were validated with WB. Further, WB showed that cabozantinib treatment inhibited p-Akt and p-MEK 1/2.

Conclusions

For the first time, we show that cabozantinib effectively inhibits viability, growth and migration of MBM cells *in vitro*. Moreover, the drug induces apoptosis and downregulates the p-RTK p-PDGF-Rα, p-IGF-1R, p-MERTK and p-DDR1 in MBM cells. Further *in vivo* experiments are needed to bring cabozantinib forward as a potential, adjuvant treatment of patients with MBM.

Introduction

Melanoma incidence rates are steadily increasing and over a third of patients with metastatic disease have brain metastases at the time of diagnosis (1). Around 40% of melanomas have a *BRAF* mutation,

most frequently *BRAF*^{V600E} (2). BRAF inhibitors like vemurafenib or dabrafenib have shown intracranial responses in most patients (3). However, responses are typically incomplete and short-lived due to intrinsic and extrinsic resistance mechanisms. Immunotherapies have also increased melanoma survival, but it remains difficult to predict response (4). Drug therapy of brain metastases is further hampered by limited drug penetration beyond the blood-brain barrier (BBB) (5, 6).

Receptor tyrosine kinases (RTK) are cell surface receptors that play important roles in regulation of gene transcription, cell proliferation and cell cycle. Consequently, mutations in RTKs can lead to altered RTK expression and development of cancer (7). Cabozantinib is an oral multi-target RTK inhibitor, which is currently FDA approved for treatment of renal, thyroid and liver cancers (8). The inhibitor has demonstrated an anti-cancer effectiveness with 55% tumour regression and 5% objective response rate in extracranial metastatic melanoma (9). Growing evidence suggests that cabozantinib may be effective against brain tumours (10–12), and there is an ongoing clinical trial on brain metastases from renal cell carcinoma (NCT03967522). Cabozantinib has repeatedly been shown to inhibit phosphorylation of RTKs such as c-Met, AXL and VEGFR (13), which are frequently dysregulated in melanomas. In this study, we report novel findings on cellular and molecular effects of cabozantinib on melanoma brain metastasis (MBM) *in vitro*.

Materials And Methods

Cell lines and cell culture

The Regional Ethical Committee (REC) approved the tissue collection, biobank storage of tumour biopsies, as well as development and use of cell lines (REC Approvals 2013/720 and 2020/65185). Written, informed consent was obtained from all patients. Cell lines were authenticated by short tandem repeat (STR) fingerprinting.

The H1, H3 and H10 cell lines were established in our laboratory from patient biopsies of MBM. The *BRAF* mutation status of the H1, H3 and H10 cell lines was determined by massive parallel sequencing of the tumour DNA, as previously described (14). The H1 and H10 cell lines are *BRAF*^{V600E} mutated, while the H3 cells are *BRAF*^{L577F} mutated.

All cells were grown in Dulbecco's Modified Eagles Medium (Sigma-Aldrich Inc., St. Louis, MO, USA, cat. #D5671), supplemented with 10% heat-inactivated new-born calf serum (ThermoFischer Scientific, Waltham, MA, USA), 5 µg/mL Plasmocin (Invivogen, Toulouse, France), 2% L-glutamine (BioWhittaker, Verviers, Belgium), penicillin (100 IU/mL) and streptomycin (100 µL/mL) (BioWhittaker). The cells were cultured in a standard tissue incubator at 37^0C, 100% humidity and 5% CO_2, and trypsinised when they attained 75% confluency using 0.25% Trypsin/EDTA (BioWhittaker).

Drug

Cabozantinib (Chemietek, Indianapolis, IN, USA, cat. #CT-XL184) was dissolved in dimethylsulfoxide (Sigma-Aldrich Inc., St. Louis, MO, USA, cat. #D2438) and stock concentrations of 200 mM were stored at -20^{0}C in aliquots.

Monolayer cell viability assay

Cell viability was studied using an MTS assay (CellTiter 96™ AQueous One Solution Cell Proliferation Assay, Promega Corporation, Fitchburg, WI, USA, cat. #G358A). Briefly, cells were seeded at a density of 5 X 10^3 cells in 200 mL culture medium per well in 96-well plates (ThermoFischer Scientific, cat. #167008). The day after, cells were left untreated to serve as control or treated with cabozantinib (0.01, 0.1, 0.5, 1, 5, 10, 20, 50 and 100 µM) for a period of 72 h. After treatment, 20 mL of the MTS solution was added into each well, and the cells were incubated for 3 h at 37^{0}C. The absorbance was measured at 492 nm using a plate reader (Multiscan FC Microplate Photometer, ThermoFischer Scientific) with SkanIt software (ThermoFischer Scientific). In each experiment, 6 wells (n = 6) were included for every control and drug concentration, and triplicate experiments were performed. Graphs were made after blank subtraction, and IC_{50} doses were calculated using GraphPad Prism version 8 (GraphPad Software, Inc., La Jolla, CA, USA). Morphology pictures were taken with a Nikon TE2000 inverted microscope (Nikon Instruments Inc., Melville, NY, USA) before MTS was added.

Tumoursphere cell viability assay

A base agar was prepared by mixing one part of 2.4% Difco Noble Agar (Becton, Dickinson and Company, Frankin Lakes, NJ, USA, cat. #214230) in sterile deionised water with three parts of culture medium at 50^{0}C in a water bath. The liquid agar was then transferred to a petri dish placed on a 50^{0}C heat block and subsequently distributed into 96-well plates (ThermoFischer Scientific, cat. #167008) at 50 mL per well using an 8-channel pipette. Cooling of the agar-coated plates was conducted in a fridge for 30 min. A soft agar solution was prepared by mixing one part of 2.4% low melting point agarose (Sigma-Aldrich Inc., cat. #A9414) in sterile deionised water with three parts of culture medium at 50°C in a water bath. The liquid agar was temporarily kept at 40°C. A suspension of 8 X 10^4 cells/mL in pre-warmed culture medium (37°C) was prepared and mixed with an equal volume of the prepared soft agar solution. The cell-containing soft agar was then transferred to a petri dish on a 37°C heat block and distributed on top of the base agar at 50 mL per well (2000 cells per well). The 96-well plates were thereafter kept in room temperature (RT) for 30 min before adding 100 mL cabozantinib (per well) at concentrations 1, 10 and 50 µM for H1; 0.5, 5 and 15 µM for H3; and 0.5, 5 and 40 µM for H10. Control cells were included in wells without addition of cabozantinib. The cells were then incubated for 14 days, and the culture medium was changed every third day. To assess colony formation, microscopy pictures were first obtained using a Nikon TE2000 inverted microscope. Thereafter, a resazurin viability assay (15) was carried out. Briefly,

20 mL of 0.1 mg/mL resazurin (Sigma-Aldrich Inc., cat. #R7017) was added to each well. Following incubation at 37^0C for 4 h, the absorbance was measured at dual mode 560/590 nm with a scanning multiwell spectrophotometer (Victor 3 1420 multi-label counter, Perkin Elmer, Waltham, MA, USA) with Workout 2.5 data analysis software. The results were prepared in GraphPad Prism version 8 (GraphPad Software, Inc.) after blank subtraction. Each experiment was performed in triplicate.

Cell migration assay

H1, H3 and H10 cells were seeded in an ImageLock 96-well plate (Essen BioScience Ltd., Hertfordshire, UK cat. #4379) at a density of 3.0 X 10^4, 2.5 X 10^4 and 3.8 X 10^4 cells per well, respectively. 48 h later, an IncuCyte wound-maker tool (Essen BioScience Ltd.) was employed to simultaneously create a uniform wound across all wells. All wells were carefully washed with preheated culture medium to remove floating cells, before adding 200 µL culture medium without or with cabozantinib (0.5, 5 and 15 µM for all cell lines) to each well. The cells were placed in an IncuCyte® Live Cell Imaging System (Essen BioScience Ltd.) and imaging was carried out every 2 h for 72 h using the 10x objective. Wound closure was analysed using the IncuCyte® Scratch Wound Cell Migration Software Module (Essen BioScience Ltd., cat. #9600-0012). Each experiment was performed in triplicate.

Apoptosis assay by flow cytometry

Apoptosis was assessed using the AlexaFluor®488 Annexin V/dead cell apoptosis kit (ThermoFischer Scientific, cat. #V13245). For all cell lines, 1.0 X 10^5 cells were seeded in 3 mL growth medium per well in a 6-well plate (ThermoFischer Scientific, cat. #140675). After 24 h of incubation, cabozantinib was added to the cells at final concentrations of 1, 10 and 50 µM for H1; 0.5, 5 and 15 µM for H3; and 0.5, 5 or 40 µM for H10 and incubated for 24, 48 or 72 h. Untreated cells were included as controls. On the day of analysis, the culture medium was transferred to separate tubes (Sarstedt, Nümbrecht, Germany, cat. #62.554.502). The cell monolayers were then washed with 500 µL PBS and washing solution was transferred into the corresponding tubes. The remaining, adherent cells were trypsinised using 0.25% Trypsin/EDTA (BioWhittaker), collected and added to its respective tube, followed by washing and centrifugation at 900 rpm for 4 min. Supernatant was discarded and 100 µL of Annexin V binding buffer containing 5 µL of Annexin V and 1 µL propidium iodide (ThermoFischer Scientific, cat. #V13245) was added to each cell pellet and incubated in the dark for 15 min at RT. The cells were analysed using a flow cytometer (BD Fortessa, BD Bioscience, San Jose, CA, USA). Fluorescence in the FITC-A and PE-A channels were gated to a two-parameter histogram, and analysed using FloJo software (Tree Star Inc., Ashland, OR, USA). The experiment was repeated three times.

Apoptosis assay by caspase 3/7 activity

Apoptosis was further assessed using the Incucyte Caspase-3/7 Red Reagent for Apoptosis (Essen BioScience Ltd., cat. #4704). For all cell lines, 1.0 X 10^4 cells in 100 mL medium were seeded per well in a 96-well plate (ThermoFischer Scientific, cat. #167008) and incubated for 24 h. The culture medium was then removed and 100 mL of preheated culture medium without or with cabozantinib (0.5, 5 or 15 μM for all cell lines) containing red apoptosis reagent was instantly added. The plate was incubated in the IncuCyte® ZOOM Live-Cell Analysis System (Essen BioScience Ltd) 30 min prior to scanning. Images for each well were carried out every 2 h for 72 h using the 10x objective, collecting one phase contrast image and one red fluorescent image each time. The IncuCyte® ZOOM Live-Cell Analysis System was used to determine the confluence and red object count. To normalise for different number of cells per well after cabozantinib treatment, data was presented as ratios of red object count to confluence. The experiment was conducted in duplicate (n=4 per experiment).

Receptor Tyrosine Kinase (RTK) Array

To elucidate the molecular effects of cabozantinib, we employed a Human Phospho-RTK (p-RTK) Array Kit (R&D Systems, Minneapolis, MN, USA, cat. #ARY001B). Briefly, H1 cells were untreated or treated with 50 μM cabozantinib for 48 h. Cells were lysed with the kit lysis buffer containing a cocktail of protease inhibitors and phosphatase inhibitors (Roche, Basel, Switzerland, cat. #4693124001 and cat. #04906837001; Tocris Bioscience, Bristol, UK, cat. #1190). The lysates were centrifuged at 14 000 g for 5 min to remove cellular debris and quantified using bicinchoninic acid (BCA) protein assay (ThermoFischer Scientific, cat. #23225). The kit arrays were blocked for 1 h before buffer was aspirated. To each array, 300 mg total protein of a cell lysate diluted in a final volume of 1.5 mL of blocking buffer was added and incubated overnight at 4°C. The arrays were washed three times with washing buffer. Anti-Phospho-Tyrosine HRP detection Antibody was diluted with the accompanying array buffer and pipetted into the two wells with the arrays. The arrays were incubated for 2 h at RT and washed twice. To develop the protein expression levels, an enhanced chemiluminescence kit (ThermoFischer Scientific, cat. #A43841) was used. The membranes were imaged with 1-10 min exposure time using the LAS3000 imaging system (FujiFilm, Saitama, Japan). ImageJ software version 2.0.0 (National Institutes of Health, Bethesda, MD, USA) quantified relative expressional levels normalised against the reference spots and presented as a ratio against negative control. The experiment was performed in triplicate.

Western blots

Western blots (WB) were performed to validate the results from the RTK arrays. H1, H3 and H10 cells were untreated controls or treated with cabozantinib at 1, 10 and 50 μM (H1); or 0.5, 5 and 15 μM (H3); or 0.5, 5 and 40 μM (H10), for 72 h. The cells were lysed using ice-cold radioimmunoprecipitation assay (RIPA)

lysis buffer (ThermoFischer Scientific, cat. #09901), supplemented with a cocktail of protease inhibitors (Roche, cat. #4693124001) and phosphatase inhibitors (Roche, cat. #04906837001). The cell lysates were centrifuged at 13 000 rpm for 5 min at 4^0C, and the resulting supernatants were used. Total protein concentration was quantified by BCA protein assay (ThermoFischer Scientific, cat. #23225), and 20 µg – 35 µg total proteins of each cell lysate were resolved by SDS-PAGE. Separated proteins on gels were transferred to nitrocellulose membranes (GE Healthcare Life Sciences, Chicago, Illinois, USA, cat. #10600001, which were subsequently blocked in Tris-Buffered Saline (TBS) containing 0.1% Tween and 5% skim-milk (blocking buffer) at RT. After washing twice in 0.1% Tween containing TBS (TBS-Tween), the membranes were incubated overnight at 4°C in blocking buffer or antibody diluent (ThermoFischer Scientific, cat. #00-3218) containing the following antibodies: phospho-PDGFR-a (Cell Signaling Technology, Inc., Danvers, MA, USA, cat. #2992), phospho-MERTK (Abcam, Cambridge, UK, cat. #14921), phospho-IGF1 (Abcam, cat. #39398), phospho-DDR1 (Cell Signaling Technology, Inc., cat. #11994), phospho-Mek 1/2 (Cell Signaling Technology, Inc., cat. #9154), phospho-Akt (Cell Signaling Technology, Inc., cat. #4056S), loading control anti-beta actin (Abcam, cat. #ab8227), loading control GAPDH (Abcam, cat. #9485). The membranes were washed five times with TBS-Tween and incubated for 1 h with 1:10000 dilution of Goat anti-Rabbit IgG (H+L) Cross-Adsorbed Secondary Antibody (Invitrogen, Waltham, MA, USA, cat. #31462) in blocking buffer. After washing the membranes 5 times, proteins were detected using an enhanced chemiluminescence kit (ThermoFischer Scientific, cat. #A43841) and LAS3000 imaging system (FujiFilm). Protein expressional levels were quantified based on density of protein bands detected using the ImageJ software version 2.0.0 (National Institutes of Health). Relative protein levels were first normalised against loading control and then calculated and presented as ratios against the untreated controls. The experiments were done in triplicate.

Statistical analysis

Differences between treatment groups were assessed using an unpaired, two-tailed T-test in either Excel version 16.45 (Microsoft) or Graphpad Prism version 8 (GraphPad Software Inc.) A P-value < 0.05 was regarded as statistically significant.

Results

MBM cell viability and colony formation is decreased after cabozantinib treatment

To examine if cabozantinib affected MBM cell growth, we performed monolayer cell viability assays on H1, H3 and H10 cell lines. Morphological changes were observed in H1 cells, which exhibited a more elongated shape upon cabozantinib treatment. H3 cell morphology appeared to be unchanged, while H10 cells became more rounded after treatment (Fig. 1a). A dose-dependent decrease in number of viable cells was observed after 72 h of treatment, with IC_{50} doses of 71.8 µM, 33.4 µM and 70.4 µM for the H1, H3 and H10 cell line, respectively (Fig. 1b).

Tumoursphere viability assays were carried out to investigate the effects of cabozantinib on colony formation and anchorage-independent growth. After 14 days of treatment, the colonies were both fewer in numbers and smaller in sizes as compared to the untreated controls (Fig. 2a). The IC_{50} values were 4.9 µM, 0.8 µM and 1.7 µM for the H1, H3 and H10 cells, respectively (Figs. 2b, 2c). Thus, MBM cells in tumourspheres were more sensitive to cabozantinib treatment than in monolayer cultures.

Cabozantinib inhibits MBM cell migration

To assess the effect of cabozantinib on tumour cell migration, we performed scratch wound assays. Cabozantinib slowed down wound closure in all cell lines in a dose dependent manner (Fig. 3a, Suppl. Movies 1a-d, 2a-d, 3a-d). A quantification of wound confluency showed that the highest cabozantinib dose resulted in a confluency of around 35% for H1 cells, and around 15% confluency for H3 and H10 cells (Fig. 3b). Hence, H1 cells were more resistant to the drug.

Cabozantinib induces apoptosis in MBM cell lines

To investigate further the observed inhibitory effects of cabozantinib on MBM cell viability and colony formation, apoptosis assays were performed. Cabozantinib induced apoptosis in H1, H3 and H10 at 50 µM, 15 µM, and 40 µM, respectively (Fig. 4, Suppl. Figs. 1a-b, 2a-b). Early apoptosis at 72h in cells treated with the specified drug dose was 20.8% in H1 cells, 14.2% in H3 cells and 18.1% in H10 cells, compared to 7.8%, 6.7% and 5.0 % in untreated cells, respectively (Fig. 4b). The results were confirmed by caspase 3/7 experiments (Suppl. Fig. 3a-b).

Cabozantinib targets a broad range of p-RTKs in MBM cells

To elucidate the molecular mechanism behind the observed effects of cabozantinib, we performed a p-RTK array. The results showed that cabozantinib treatment led to reduced expression of several phosphorylated RTKs in H1 cells. Particularly, p-IGF-1R, p-MERTK and p-DDR1 displayed the most significant reduction, whereas p-PDGF-Ra protein expression was not significantly decreased (Fig. 5, Suppl. Fig. 4).

To verify these results, WBs for p-PDGF-Ra, p-IGF-1R, p-MERTK and p-DDR1 were performed on lysates of cabozantinib-treated and untreated cells. All the p-RTKs showed a dose-dependent downregulation in their protein expression across all cell lines after cabozantinib treatment (Fig. 6). Downregulation was generally most pronounced in H10 cells and least in H1 cells. The p-PDGF-Ra was modestly downregulated in H1 and H3 cells, while p-MERK and p-IGF-1R showed a higher degree of downregulation in all cell lines. The highest reduction in protein expression levels were observed in p-DDR1 in H3 and H10 cells.

MAPK and PI3K-Akt signalling pathways in MBM cells are affected by cabozantinib

To assess the impact of cabozantinib on the critical MAPK and PI3K-Akt signalling pathways, we performed WBs on key proteins of the pathways. We found that p-MEK 1/2 was inhibited in H1 and H10

cells, and seemingly unaffected in H3 cells (Fig. 7). Further, p-Akt protein level was decreased in H1 and H10 cells, while it had a trend towards an increase in H3 cells after treatment (Fig. 7).

Discussion

Targeted therapy and immunotherapy are key components of contemporary melanoma treatment. These treatments are however hampered by resistance problems and exert relatively poor effects on brain metastases, necessitating new, adjuvant treatments of MBM patients. In this study, we report for the first time inhibitory effects of the multi-target RTK inhibitor cabozantinib in a panel of MBM cell lines *in vitro*.

The IC_{50} values of cabozantinib-treated monolayers were comparable to previous reports (16–19). Tumourspheres are regarded as more representative to solid tumour growth *in vivo* (20, 21). Cabozantinib inhibited tumoursphere growth for all cell lines (Fig. 2). The IC_{50} doses were only 2.4–6.8% of the IC_{50} doses found in the monolayer experiments. This is a common finding (22) and suggests that MBM cells may be more sensitive to treatment when grown in an anchorage-independent microenvironment.

It is well known that melanoma has an elevated capacity of migration and invasion compared to other solid tumours, and historic autopsy studies have found brain metastases in more than 70% of melanoma patients (23). In the present study, exposure to cabozantinib showed a dose dependent inhibition of cell migration (Fig. 3). Drug doses much lower than IC_{50} doses were able to inhibit migration, similar to findings from other studies (24). Taken together, the viability and migration results imply that cabozantinib may inhibit cell migration at low doses, even when cell proliferation is not altered.

Resistance to regulated cell death plays a vital role in carcinogenesis, including melanoma (25). Initiation of the apoptotic cascade leads to activation of the enzyme caspase-3, resulting in DNA breakage and cytomorphological changes (26). In the current study, cabozantinib induced early apoptosis in 14–21% of the cells after 72 h treatment, also leading to upregulation of caspase-3/7 (Fig. 4b, Suppl. Figure 3a-b).

To elucidate how cabozantinib increased apoptosis, we performed a p-RTK array analysis which showed a broad inhibition of protein expression levels after treatment (Fig. 5). Our studies indicate that downregulated expression levels of p-PDGF-Rα, p-IGF-1R, p-MERTK and p-DDR1 induce apoptosis in MBM cell lines (Fig. 6), however the contribution of other p-RTKs cannot be ruled out. Gene deletion of PDGF-Ra has previously been shown to trigger apoptosis (27) and the ligand IGF is found to be an apoptosis regulator (28). Interestingly, phagocytosis of apoptotic cells is mediated by MERTK in macrophages (29), while DDR1 induces apoptosis trough upregulation of pro-apoptotic tumour suppressors (30).

Targeting these four p-RTKs makes sense from a clinical point of view. Melanoma derived PDGF upregulates the hyaluronic acid production in fibroblasts, which in turn stimulates melanoma proliferation (31). Moreover, it is indicated that IGF-1R expression in melanoma is regulated by surrounding stromal cells, as well as PTEN and BRAF status (32). A clinical drug combination study in hepatocellular carcinoma is ongoing, due to the immunosuppressive effects of cabozantinib on the tumour microenvironment (33). MERTK expression is correlated with melanoma disease progression (34)

and suppression of MERTK is found to inhibit melanoma cell proliferation and migration *in vitro* (35). The receptor DDR1 acts as an adhesion molecule in normal melanocytes and contributes to cellular homeostasis (36). Elevated expression of DDR1 in melanoma is associated with a poor prognosis and downregulation of DDR1 inhibits migration, invasion, and survival of melanoma cells (37, 38). To the best of our knowledge, it has never been documented that cabozantinib is able to inhibit p-DDR1. Yet, cabozantinib have been proposed to inhibit DDR1 in prostate cancer (39).

The MAPK and PI3K/Akt signalling pathways are frequently upregulated in MBM. Activation of these pathways typically occurs through phosphorylation of RTKs leading to increased intracellular signalling (40, 41). The $BRAF^{V600E}$ mutation drives constitutive activation of the MAPK pathway through among others p-MEK 1/2 (42). The expression of p-Akt increases with melanoma invasion and progression and is correlated with poor patient survival (43).

We showed that cabozantinib treatment inhibited p-MEK 1/2 and p-Akt expression in the $BRAF^{V600E}$ mutated cell lines H1 and H10 (Fig. 7). This is consistent with findings from non-BRAF mutated cancers (16, 44). In the $BRAF^{L577F}$ mutated H3 cell line, p-MEK 1/2 and p-Akt did not seem to be affected by cabozantinib. Yet, increased apoptosis was seen after treatment of all cell lines, including H3. Thus, other signalling pathways than PI3K-Akt and MAPK are likely involved in the induction of apoptosis after cabozantinib treatment. For example, the WNT pathway can also be aberrated in melanoma (45). Interestingly, unpublished data from our lab shows that H3 harbours a mutation in the WNT pathway, more specifically in the APC gene. NRAS upstream in both MAPK and PI3K pathways is also mutated in H3. Cross-talk between the WNT and MAPK signalling pathways have been documented due to APC loss and KRAS mutation in intestinal cancer (46). Constitutive activation of NRAS may also explain the lack of downregulation of p-MEK 1/2 and p-Akt in H3, however this was not investigated further in our work. Moreover, RTKs can interact directly with other RTKs (47–49). For instance, DDR1 overexpression enhances Akt and Erk1/2 activation in response to IGF-1 (50). Altogether, one could speculate that crosstalk exaggerated apoptosis in H3 upon cabozantinib treatment, independently of p-MEK 1/2 and p-Akt expression.

In our study, the cell lines did not possess mutations of the RTKs which were found to be downregulated. To enhance clinical relevance, further cabozantinib studies using selective RTK^{-}/RTK^{+} cell lines would be warranted. Also, the clinical applicability of cabozantinib would increase if the drug is proven effective in combination with BRAF inhibitors.

Conclusions

We show for the first time that cabozantinib decreases cell viability, colony formation, anchorage independent cell growth and migration in human MBM cells *in vitro*. The drug also induces apoptosis through inhibited expression of the p-RTKs p-PDGF-Ra, p-IGF-1R, p-MERTK and p-DDR1. Further, cabozantinib inhibits p-Akt and p-MEK 1/2. Additional *in vivo* studies are warranted, to provide data for future translational use of cabozantinib in the treatment of patients with MBM.

Declarations

Acknowledgements

All **imaging** *was performed at the Molecular Imaging Center, Department of Biomedicine, University of Bergen.* The flow cytometry was performed at the Flow Cytometry Core Facility, Department of Clinical Science, University of Bergen.

Funding

The study was funded by The Norwegian Cancer Society (grant no 182716), The Western Regional Health Authority (grant no F-11970), the University of Bergen and The Medical Student Research Programme at The Faculty of Medicine, University of Bergen. The funders had no role in study design, data collection and analysis, decision to publish, or preparation of the manuscript.

Availability of data and materials

The datasets used and analysed during the current study are available from the corresponding author on reasonable request.

Author´s contributions

Conception and design: FT, TAM; Development of methodology: TH, SNA, OVB, TAM, HP; Execution and Analysis: TAM, TH; Writing, reviewing and/or revision of manuscript: TAM, FT, TS, TH, SNA, OVB, HP

Ethics approval and consent to participate

The Regional Ethical Committee (REC) approved tissue collection, biobank storage of tumour biopsies, as well as development and use of cell lines (REC Approvals 2013/720 and 2020/65185).

Consent for publication

Not applicable.

Competing interests

The authors declare that they have no competing interests.

Abbreviations

BRAF: v-Raf murine sarcoma viral oncogene homolog B1

BBB: Blood-brain barrier

RTK: Receptor tyrosine kinase

FDA: The United States Food and Drug Administration

C-met: Mesenchymal-epithelial transition factor

VEGFR: Vascular endothelial growth factor receptor

MBM: Melanoma brain metastasis

REC: The Regional Ethical Committee

STR: Short tandem repeat

EDTA: Ethylenediamine tetraacetic acid

MTS: 3-(4,5-dimethylthiazol-2-yl)-5-(3-carboxymethoxyphenyl)-2-(4-sulfophenyl)-2H-tetrazolium, inner salt

IC_{50}: Half maximal inhibitory concentration

RT: Room temperature

PBS: Phosphate buffered saline

p-RTK: Phosphorylated-RTK

BCA: Bicinchoninic acid

HRP: Horseradish peroxidase

WB: Western Blot

RIPA: Radioimmunoprecipitation assay

SDS-PAGE: Sodium dodecyl sulfate-polyacrylamide gel electrophoresis

TBS: Tris-Buffered Saline

PDGF-Ra: Platelet-derived growth factor-receptor a

MERTK: Mer tyrosine kinase

IGF-1R: Insulin-like growth factor 1 receptor

DDR1: Discoidin domain receptor 1

GAPDH: Glyceraldehyde 3-phosphate dehydrogenase

MAPK: Mitogen-activated protein kinase

PI3K: Phosphoinositide 3-kinase

Akt: Protein kinase B

MEK 1/2: Dual specificity mitogen-activated protein kinase kinase 1/2

PTEN: Phosphatase and tensin homolog

APC: Adenomatous polyposis coli

NRAS: Neuroblastoma Rat sarcoma protein

KRAS: Kirsten Rat sarcoma protein

Erk1/2: Extracellular-signal-regulated kinase 1/2

References

1. Zhang D, Wang Z, Shang D, Yu J, Yuan S. Incidence and prognosis of brain metastases in cutaneous melanoma patients: a population-based study. Melanoma Res. 2019;29(1):77-84.

2. Lee JH, Choi JW, Kim YS. Frequencies of BRAF and NRAS mutations are different in histological types and sites of origin of cutaneous melanoma: a meta-analysis. Br J Dermatol. 2011;164(4):776-84.

3. Davies MA, Saiag P, Robert C, Grob JJ, Flaherty KT, Arance A, et al. Dabrafenib plus trametinib in patients with BRAF(V600)-mutant melanoma brain metastases (COMBI-MB): a multicentre, multicohort, open-label, phase 2 trial. Lancet Oncol. 2017;18(7):863-73.

4. Fattore L, Ruggiero CF, Liguoro D, Castaldo V, Catizone A, Ciliberto G, et al. The Promise of Liquid Biopsy to Predict Response to Immunotherapy in Metastatic Melanoma. Front Oncol. 2021;11:645069.

5. Mittapalli RK, Vaidhyanathan S, Dudek AZ, Elmquist WF. Mechanisms Limiting Distribution of the Threonine-Protein Kinase B-RaF^{V600E} Inhibitor Dabrafenib to the Brain: Implications for the

Treatment of Melanoma Brain Metastases. Journal of Pharmacology and Experimental Therapeutics. 2013;344(3):655-64.

6. Gampa G, Vaidhyanathan S, Sarkaria JN, Elmquist WF. Drug delivery to melanoma brain metastases: Can current challenges lead to new opportunities? Pharmacol Res. 2017;123:10-25.

7. Lemmon MA, Schlessinger J. Cell signaling by receptor tyrosine kinases. Cell. 2010;141(7):1117-34.

8. National Cancer Institute. FDA approvals for cabozantinib. Accessed 09 December 2020 [Available from: https://www.cancer.gov/about-cancer/treatment/drugs/cabozantinib-s-malate.

9. Daud A, Kluger HM, Kurzrock R, Schimmoller F, Weitzman AL, Samuel TA, et al. Phase II randomised discontinuation trial of the MET/VEGF receptor inhibitor cabozantinib in metastatic melanoma. Br J Cancer. 2017;116(4):432-40.

10. Négrier S, Moriceau G, Attignon V, Haddad V, Pissaloux D, Guerin N, et al. Activity of cabozantinib in radioresistant brain metastases from renal cell carcinoma: two case reports. J Med Case Rep. 2018;12(1):351.

11. Sun TY, Niu X, Chakraborty A, Neal JW, Wakelee HA. Lengthy Progression-Free Survival and Intracranial Activity of Cabozantinib in Patients with Crizotinib and Ceritinib-Resistant ROS1-Positive Non-Small Cell Lung Cancer. J Thorac Oncol. 2019;14(2):e21-e4.

12. Wen PY, Drappatz J, de Groot J, Prados MD, Reardon DA, Schiff D, et al. Phase II study of cabozantinib in patients with progressive glioblastoma: subset analysis of patients naive to antiangiogenic therapy. Neuro-oncology. 2018;20(2):249-58.

13. Yakes FM, Chen J, Tan J, Yamaguchi K, Shi Y, Yu P, et al. Cabozantinib (XL184), a novel MET and VEGFR2 inhibitor, simultaneously suppresses metastasis, angiogenesis, and tumor growth. Mol Cancer Ther. 2011;10(12):2298-308.

14. Bischof K, Knappskog S, Hjelle SM, Stefansson I, Woie K, Salvesen HB, et al. Influence of p53 Isoform Expression on Survival in High-Grade Serous Ovarian Cancers. Scientific Reports. 2019;9(1):5244.

15. Riss TL, Moravec RA, Niles AL, Duellman S, Benink HA, Worzella TJ, et al. Cell Viability Assays. In: Markossian S, Sittampalam GS, Grossman A, Brimacombe K, Arkin M, Auld D, et al., editors. Assay Guidance Manual. Bethesda (MD): Eli Lilly & Company and the National Center for Advancing Translational Sciences; 2004.

16. Shang R, Song X, Wang P, Zhou Y, Lu X, Wang J, et al. Cabozantinib-based combination therapy for the treatment of hepatocellular carcinoma. Gut. 2020.

17. Dong Y, Hu H, Sun Y, Qin M, Gong P, Hou Y, et al. Design, synthesis and biological evaluation of novel c-Met/HDAC dual inhibitors. Bioorganic & medicinal chemistry letters. 2020;30(23):127610.

18. Starenki D, Sosonkina N, Hong SK, Lloyd RV, Park JI. Mortalin (GRP75/HSPA9) Promotes Survival and Proliferation of Thyroid Carcinoma Cells. Int J Mol Sci. 2019;20(9).

19. Zhang L, Scorsone K, Woodfield SE, Zage PE. Sensitivity of neuroblastoma to the novel kinase inhibitor cabozantinib is mediated by ERK inhibition. Cancer chemotherapy and pharmacology. 2015;76(5):977-87.

20. Duval K, Grover H, Han L-H, Mou Y, Pegoraro AF, Fredberg J, et al. Modeling Physiological Events in 2D vs. 3D Cell Culture. Physiology (Bethesda). 2017;32(4):266-77.

21. Borowicz S, Van Scoyk M, Avasarala S, Karuppusamy Rathinam MK, Tauler J, Bikkavilli RK, et al. The soft agar colony formation assay. J Vis Exp. 2014(92):e51998.

22. Sundstrøm T, Prestegarden L, Azuaje F, Aasen SN, Røsland GV, Varughese JK, et al. Inhibition of mitochondrial respiration prevents BRAF-mutant melanoma brain metastasis. Acta Neuropathol Commun. 2019;7(1):55.

23. Patel JK, Didolkar MS, Pickren JW, Moore RH. Metastatic pattern of malignant melanoma. A study of 216 autopsy cases. Am J Surg. 1978;135(6):807-10.

24. Xiang Q, Chen W, Ren M, Wang J, Zhang H, Deng DY, et al. Cabozantinib suppresses tumor growth and metastasis in hepatocellular carcinoma by a dual blockade of VEGFR2 and MET. Clin Cancer Res. 2014;20(11):2959-70.

25. Broussard L, Howland A, Ryu S, Song K, Norris D, Armstrong CA, et al. Melanoma Cell Death Mechanisms. Chonnam Med J. 2018;54(3):135-42.

26. Cavalcante GC, Schaan AP, Cabral GF, Santana-da-Silva MN, Pinto P, Vidal AF, et al. A Cell's Fate: An Overview of the Molecular Biology and Genetics of Apoptosis. Int J Mol Sci. 2019;20(17).

27. Qian C, Wu Z, Ng RC, Garcia-Barceló MM, Yuan ZW, Wong KKY, et al. Conditional deletion of platelet derived growth factor receptor alpha (Pdgfra) in urorectal mesenchyme causes mesenchyme apoptosis and urorectal developmental anomalies in mice. Cell Death Differ. 2019;26(8):1396-410.

28. Kooijman R. Regulation of apoptosis by insulin-like growth factor (IGF)-I. Cytokine Growth Factor Rev. 2006;17(4):305-23.

29. Scott RS, McMahon EJ, Pop SM, Reap EA, Caricchio R, Cohen PL, et al. Phagocytosis and clearance of apoptotic cells is mediated by MER. Nature. 2001;411(6834):207-11.

30. Assent D, Bourgot I, Hennuy B, Geurts P, Noël A, Foidart JM, et al. A membrane-type-1 matrix metalloproteinase (MT1-MMP)-discoidin domain receptor 1 axis regulates collagen-induced apoptosis in breast cancer cells. PloS one. 2015;10(3):e0116006.

31. Willenberg A, Saalbach A, Simon JC, Anderegg U. Melanoma cells control HA synthesis in peritumoral fibroblasts via PDGF-AA and PDGF-CC: impact on melanoma cell proliferation. J Invest Dermatol. 2012;132(2):385-93.

32. Wang J, Sinnberg T, Niessner H, Dölker R, Sauer B, Kempf WE, et al. PTEN regulates IGF-1R-mediated therapy resistance in melanoma. Pigment Cell Melanoma Res. 2015;28(5):572-89.

33. Kelley RK, J WO, Hazra S, Benzaghou F, Yau T, Cheng AL, et al. Cabozantinib in combination with atezolizumab versus sorafenib in treatment-naive advanced hepatocellular carcinoma: COSMIC-312 Phase III study design. Future Oncol. 2020;16(21):1525-36.

34. Schlegel J, Sambade MJ, Sather S, Moschos SJ, Tan AC, Winges A, et al. MERTK receptor tyrosine kinase is a therapeutic target in melanoma. J Clin Invest. 2013;123(5):2257-67.

35. Tworkoski KA, Platt JT, Bacchiocchi A, Bosenberg M, Boggon TJ, Stern DF. MERTK controls melanoma cell migration and survival and differentially regulates cell behavior relative to AXL. Pigment Cell Melanoma Res. 2013;26(4):527-41.

36. Fukunaga-Kalabis M, Martinez G, Liu ZJ, Kalabis J, Mrass P, Weninger W, et al. CCN3 controls 3D spatial localization of melanocytes in the human skin through DDR1. J Cell Biol. 2006;175(4):563-9.

37. Reger de Moura C, Battistella M, Sohail A, Caudron A, Feugeas JP, Podgorniak MP, et al. Discoidin domain receptors: A promising target in melanoma. Pigment Cell Melanoma Res. 2019;32(5):697-707.

38. Romayor I, Badiola I, Olaso E. Inhibition of DDR1 reduces invasive features of human A375 melanoma, HT29 colon carcinoma and SK-HEP hepatoma cells. Cell Adh Migr. 2020;14(1):69-81.

39. Vaishampayan UN, Podgorski I, Heilbrun LK, Lawhorn-Crews JM, Dobson KC, Boerner J, et al. Biomarkers and Bone Imaging Dynamics Associated with Clinical Outcomes of Oral Cabozantinib Therapy in Metastatic Castrate-Resistant Prostate Cancer. Clin Cancer Res. 2019;25(2):652-62.

40. McKay MM, Morrison DK. Integrating signals from RTKs to ERK/MAPK. Oncogene. 2007;26(22):3113-21.

41. Haddadi N, Lin Y, Travis G, Simpson AM, Nassif NT, McGowan EM. PTEN/PTENP1: 'Regulating the regulator of RTK-dependent PI3K/Akt signalling', new targets for cancer therapy. Molecular cancer. 2018;17(1):37.

42. Devji T, Levine O, Neupane B, Beyene J, Xie F. Systemic Therapy for Previously Untreated Advanced BRAF-Mutated Melanoma: A Systematic Review and Network Meta-Analysis of Randomized Clinical

Trials. JAMA Oncol. 2017;3(3):366-73.

43. Dai DL, Martinka M, Li G. Prognostic significance of activated Akt expression in melanoma: a clinicopathologic study of 292 cases. Journal of clinical oncology : official journal of the American Society of Clinical Oncology. 2005;23(7):1473-82.

44. Yang S, Zhang X, Qu H, Qu B, Yin X, Zhao H. Cabozantinib induces PUMA-dependent apoptosis in colon cancer cells via AKT/GSK-3β/NF-κB signaling pathway. Cancer Gene Ther. 2020;27(5):368-77.

45. Gajos-Michniewicz A, Czyz M. WNT Signaling in Melanoma. Int J Mol Sci. 2020;21(14).

46. Jeong WJ, Ro EJ, Choi KY. Interaction between Wnt/β-catenin and RAS-ERK pathways and an anti-cancer strategy via degradations of β-catenin and RAS by targeting the Wnt/β-catenin pathway. NPJ Precis Oncol. 2018;2(1):5.

47. Bergström JD, Westermark B, Heldin NE. Epidermal growth factor receptor signaling activates met in human anaplastic thyroid carcinoma cells. Exp Cell Res. 2000;259(1):293-9.

48. Janssen J. New Insights from IGF-IR Stimulating Activity Analyses: Pathological Considerations. Cells. 2020;9(4).

49. Vella V, Malaguarnera R, Nicolosi ML, Morrione A, Belfiore A. Insulin/IGF signaling and discoidin domain receptors: An emerging functional connection. Biochim Biophys Acta Mol Cell Res. 2019;1866(11):118522.

50. Malaguarnera R, Nicolosi ML, Sacco A, Morcavallo A, Vella V, Voci C, et al. Novel cross talk between IGF-IR and DDR1 regulates IGF-IR trafficking, signaling and biological responses. Oncotarget. 2015;6(18):16084-105.

Figures

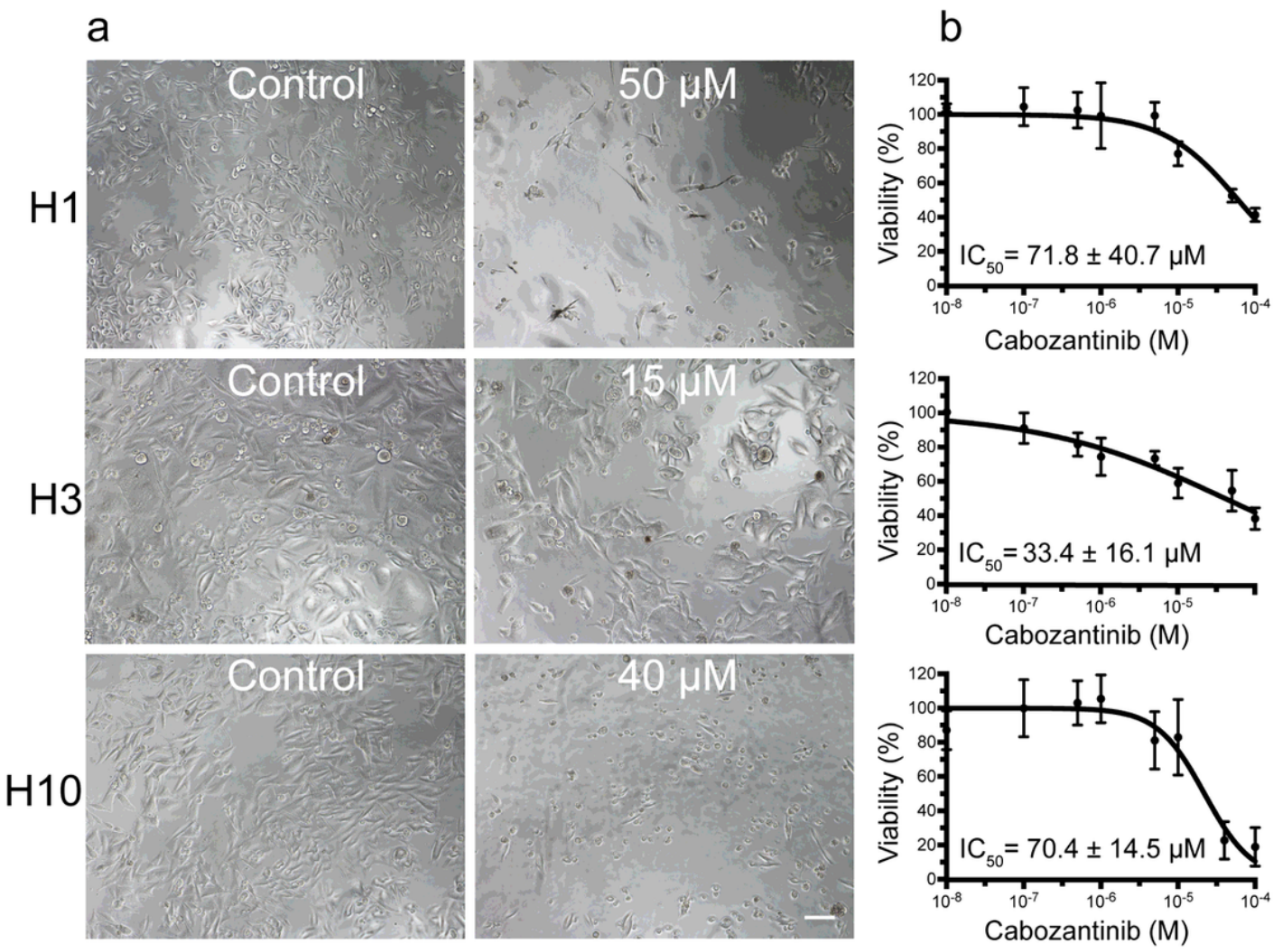

Figure 1

Cabozantinib decreases the viability of MBM cell lines in monolayer cultures. a Phase-contrast microscopic images (10x objective) of cells grown as monolayers, either untreated (control) or treated with 50 μM (H1), 15 μM (H3) or 40 μM (H10) cabozantinib for 72 h. Scale bar = 100 μm. b Representative viability curves of cells grown as monolayers after treatment with cabozantinib with increasing concentrations. The cabozantinib concentrations at which cell viability is reduced to 50% as compared to the control (IC50) were calculated from triplicate experiments.

Fig. 2

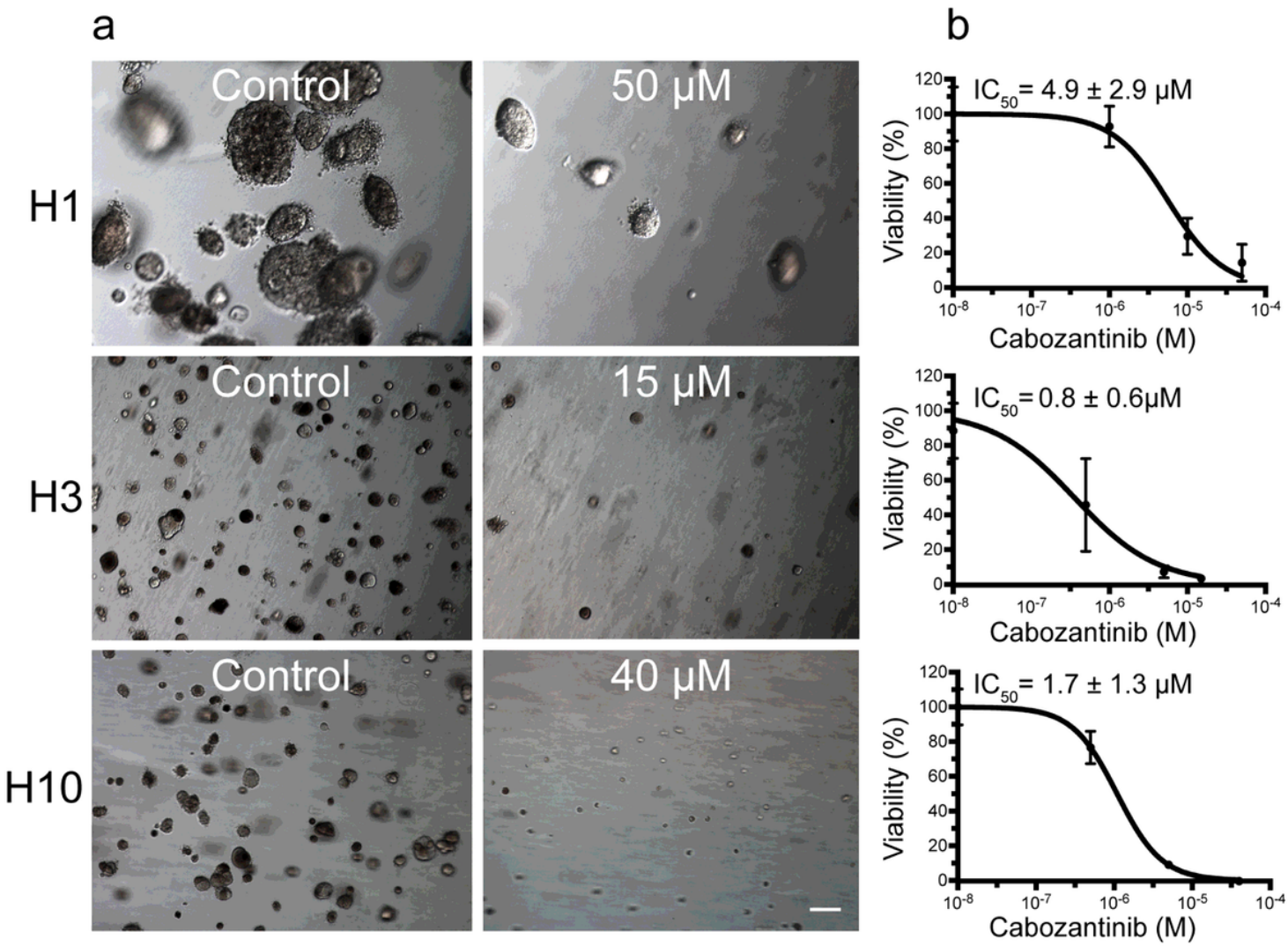

c

Cell line	Monolayer [μM]	Tumoursphere [μM]
H1	71.8 ± 40.7	4.9 ± 2.9
H3	33.4 ± 16.1	0.8 ± 0.6
H10	70.4 ± 14.5	1.7 ± 1.3

Figure 2

Cabozantinib inhibits colony formation and anchorage-independent growth in MBM cell lines. a Representative phase-contrast images (10x objective) at day 14 of H1, H3 and H10 colonies grown in soft agar, either untreated (control) or treated with 50 μM (H1), 15 μM (H3) or 40 μM (H10) cabozantinib. Scale bar = 100 μm. b Representative viability curves of cells grown as 3D cultures after treatment with cabozantinib with increasing doses. c Table showing the calculated IC50 values of cabozantinib in monolayer cell viability assays and tumoursphere cell viability assays.

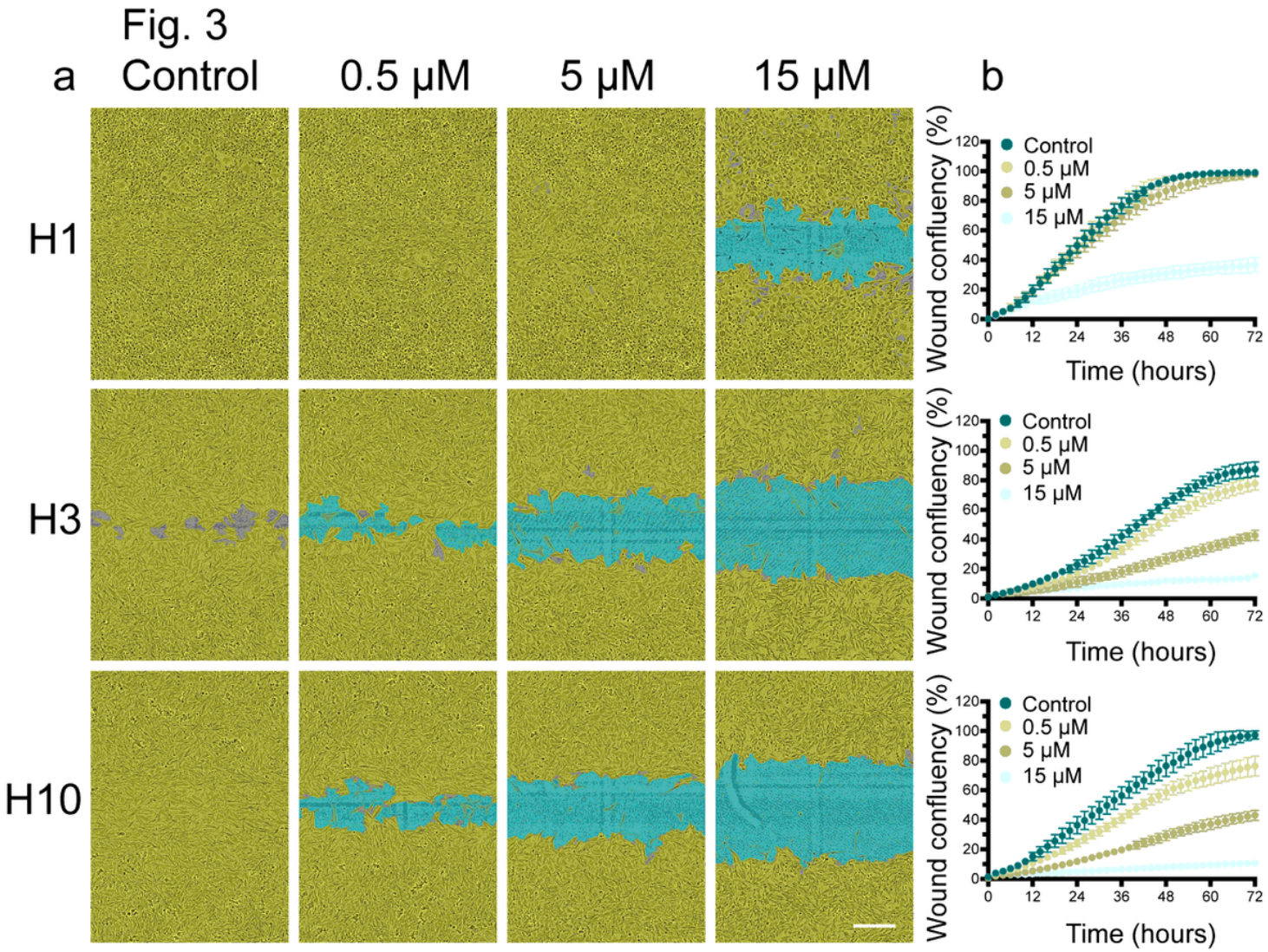

Figure 3

Cabozantinib inhibits migration of MBM cell lines. a Representative phase-contrast images (10x objective) of cells, showing the wound confluency, obtained 72 h after scratch wound and treatment with cabozantinib (0.5 μM, 5 μM or 15 μM). Control cells were untreated. Cells are coloured in yellow, and the scratch wound is coloured in blue. Scale bar = 300 μm. b Representative graphs showing wound confluency over a time period of 72 h.

Fig. 4

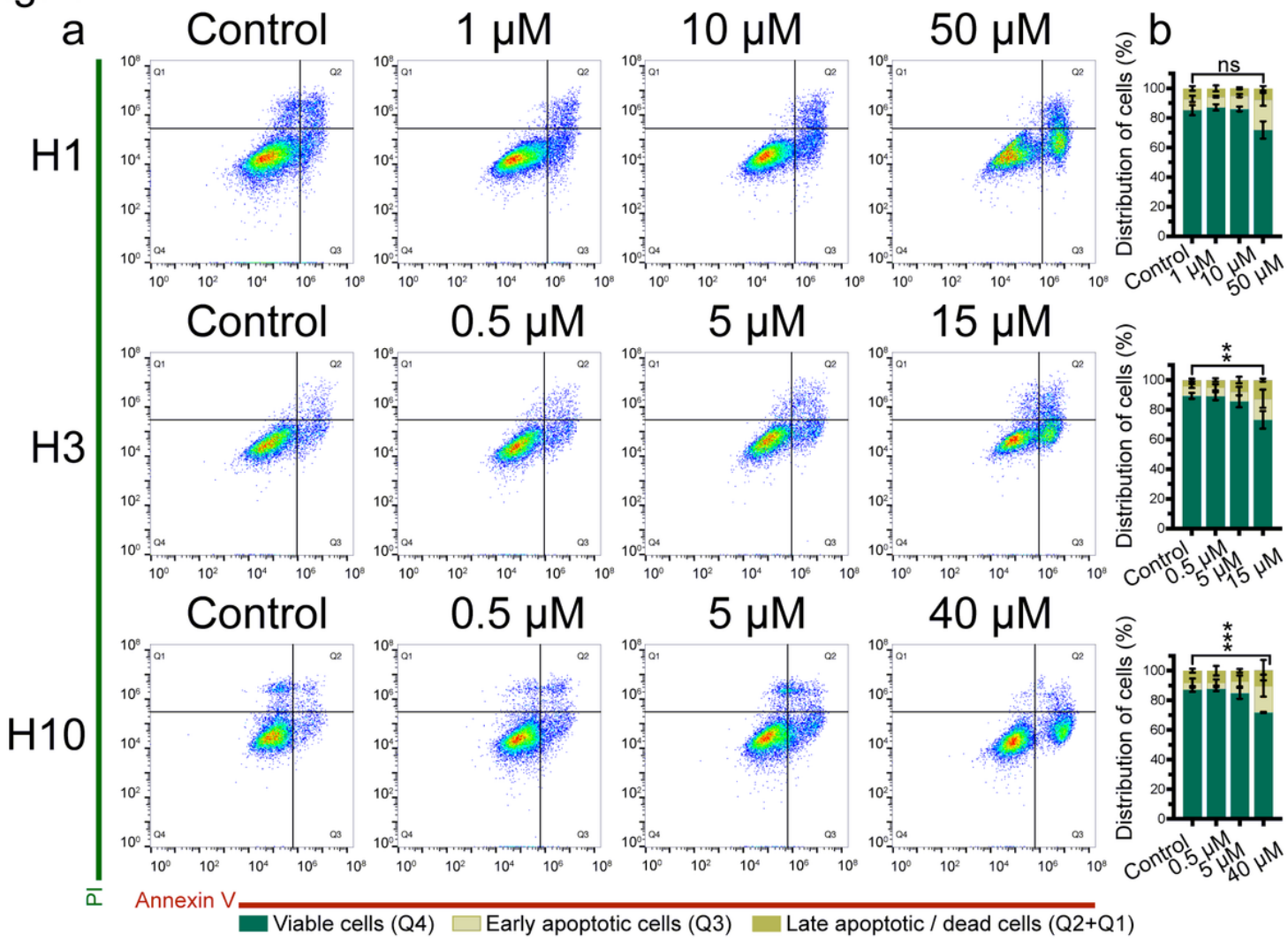

Figure 4

Cabozantinib induces apoptosis in MBM cell lines. a Representative dot plots of cells untreated (control) or treated with different doses of cabozantinib as indicated for 72 h. Annexin V labels apoptotic cells, while propidium iodide (PI) labels necrotic cells. b Quantification of the percentage of viable, apoptotic and necrotic cells in H1, H3 and H10 cell cultures as untreated (control) or after exposure to cabozantinib. The experiments were done in triplicate. Abbreviations: Q1: necrotic cells, Q2: late apoptotic cells, Q3: early apoptotic cells, Q4: viable cells. Abbreviations: ns: not significant, **: $p < 0.01$ in late apoptotic cells between control and cells treated with highest drug dose, ***: $p < 0.001$ in viable cells between control and cells treated with highest drug dose.

Fig. 5

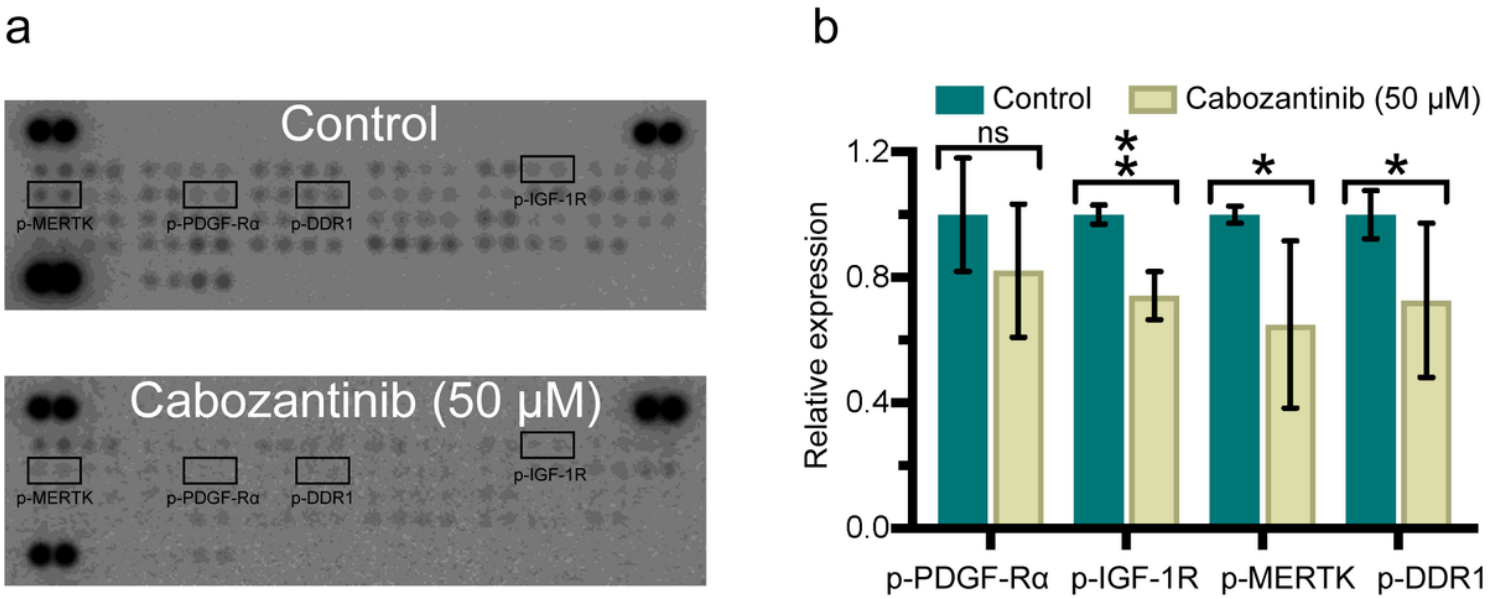

Figure 5

Multiple p-RTKs are downregulated in H1 cells after cabozantinib treatment. a Representative images of RTK arrays that were incubated with lysates of H1 cells untreated (control) or treated with 50 μM cabozantinib for 48 h. Darker spots represent higher expressional level of the p-RTKs. In each array, each p-RTK is presented by 2 spots. b Graphic presentation of expression levels of selected p-RTKs, normalised against the reference spots and presented as a ratio against the controls. Abbreviations: ns: not significant, *: $p < 0.05$, **: $p < 0.01$.

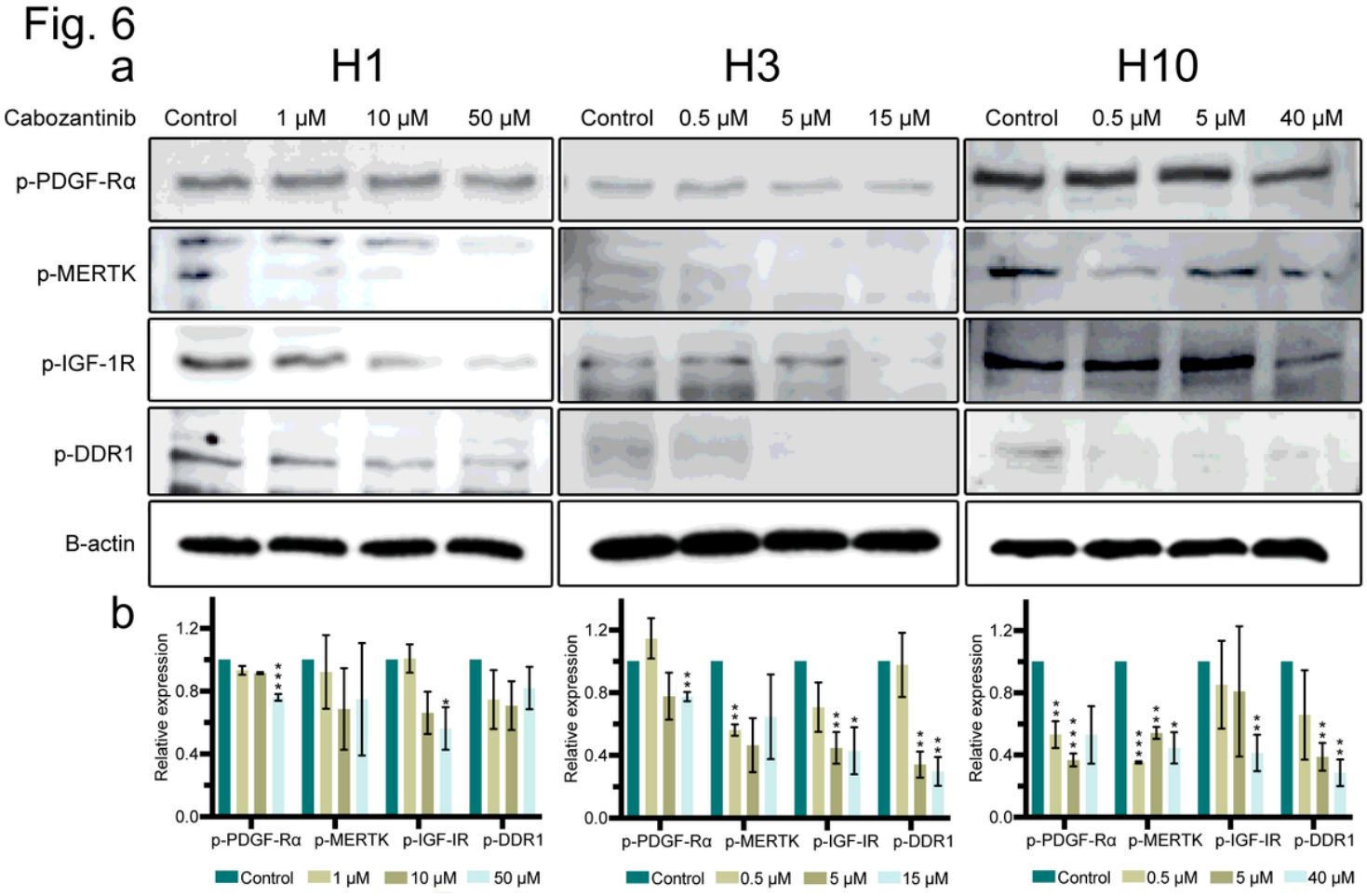

Figure 6

Cabozantinib downregulates expression of p-PDGF-Ra, p-IGF-1R, p-MERTK and p-DDR1 in MBM cell lines. a Western blots showing selected p-RTKs in H1, H3 and H10 cells untreated (control), or treated with 1 μM, 10 μM or 50 μM (H1), 0.5 μM, 5 μM, 15 μM (H3) and 0.5 μM, 5 μM, 40 μM (H10) cabozantinib for 72 h. b Quantification of target proteins detected in Western blots. Expression levels of target proteins were normalised against b-actin and compared relatively as ratio to the control for each specific protein. The Western blot experiments were performed in triplicate. Full-length blots are presented in Suppl. Fig. 5a. Abbreviations: *: $p < 0.05$, **: $p < 0.01$, ***: $p < 0.001$

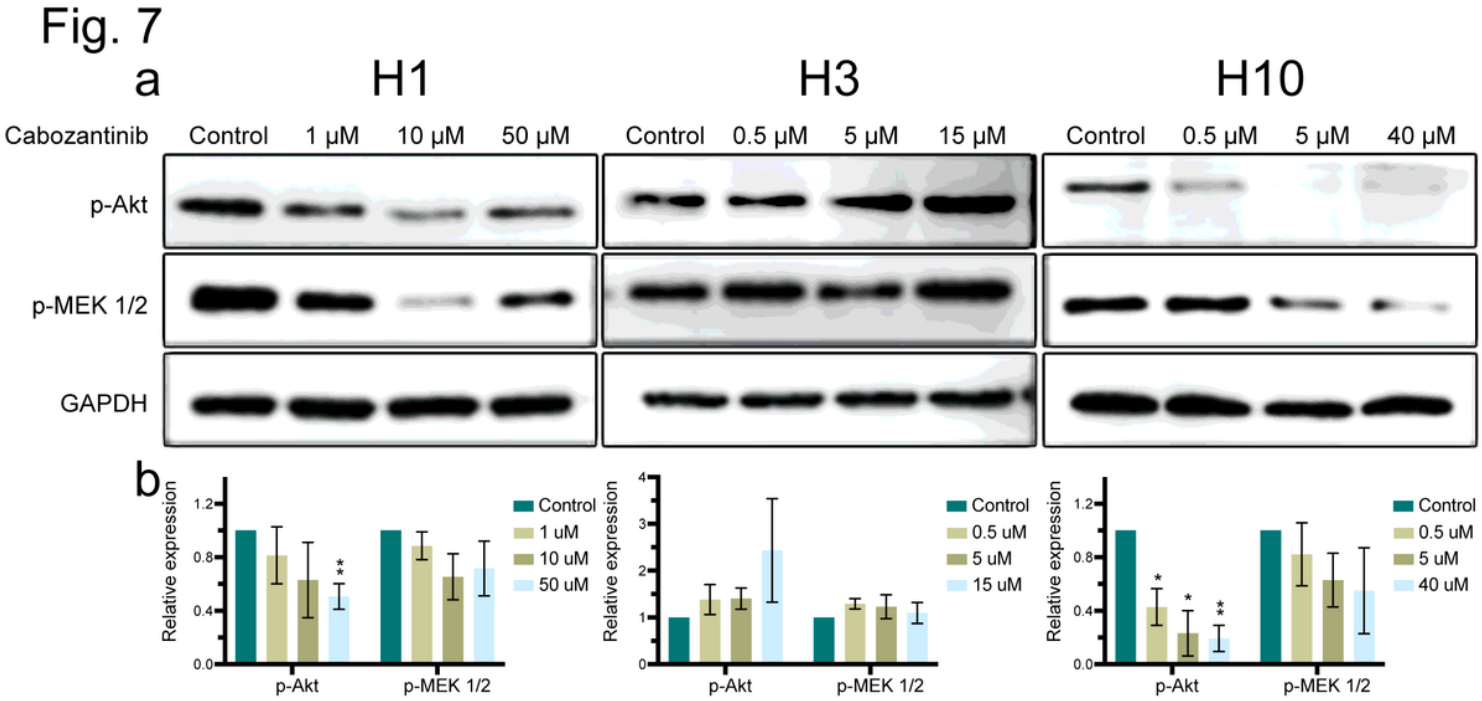

Figure 7

p-Akt and p-MEK 1/2 protein expression levels are downregulated after cabozantinib treatment. a Western blots showing the expression levels of p-Akt and p-MEK 1/2 after treatment with 1 μM, 10 μM or 50 μM (H1), 0.5 μM, 5 μM, 15 μM (H3) and 0.5 μM, 5 μM, 40 μM (H10) cabozantinib for 72 h, compared to untreated (control) cells. The Western Blot experiments were performed in triplicate. b Quantification of target proteins detected in Western blots. Expression level of target proteins were normalised against GAPDH and compared relatively as ratio to the control for each specific protein. The Western blot experiments were performed in triplicate. Full-length blots are presented in Suppl. Fig. 5b. Abbreviations: *: $p < 0.05$, **: $p < 0.01$.

Supplementary Files

This is a list of supplementary files associated with this preprint. Click to download.

- Suppl.Movie1aControlH1.mp4
- Suppl.Movie1aControlH1.mp4
- Suppl.Movie1c5uMH1.mp4
- Suppl.Movie1b0.5uMH1.mp4
- Suppl.Movie1c5uMH1.mp4
- Suppl.Movie1d15uMH1.mp4
- Suppl.Movie2d15uMH3.mp4
- Suppl.Movie3aControlH10.mp4

- Suppl.Movie3b0.5uMH10.mp4
- Suppl.Movie3c5uMH10.mp4
- Suppl.Movie3d15uMH10.mp4
- Suppl.Movie3c5uMH10.mp4
- Suppl.Movie3d15uMH10.mp4
- Suppl.Movie3b0.5uMH10.mp4
- Suppl.Movie3d15uMH10.mp4
- Suppl.Movie3d15uMH10.mp4
- Suppl.Movie3aControlH10.mp4
- Suppl.Movie2d15uMH3.mp4
- Suppl.Movie2c5uMH3.mp4
- Suppl.Movie2b0.5uMH3.mp4
- Suppl.Movie2d15uMH3.mp4
- Suppl.Movie2aControlH3.mp4
- Suppl.Movie2c5uMH3.mp4
- Suppl.Movie2b0.5uMH3.mp4
- Suppl.Movie2b0.5uMH3.mp4
- Suppl.Movie2aControlH3.mp4
- Suppl.Movie1d15uMH1.mp4
- Suppl.Movie1d15uMH1.mp4
- Suppl.Movie1c5uMH1.mp4
- Suppl.Movie1b0.5uMH1.mp4
- SupplementaryMaterial.docx